Thermophysics and Aeromechanics, *2016*, *Vol. 23*, *No. 3*

DOI: 10.1134/S0869864316030136

Entropy production in the flow over a swirling stretchable cylinder

S. Munawar[1,2], N. Saleem[3], and A. Mehmood[4]

[1]*University of Dammam*, *Dammam*, *Saudi Arabia*

[2]*University of Management and Technology*, *Lahore*, *Pakistan*

[3]*Prince Mohammad Bin Fahd University*, *Alkhubar*, *Saudi Arabia*

[4]*International Islamic University Islamabad*, *Pakistan*

E-mail: sufian.munawar@hotmail.com

(*Received April 2*, *2015*; *in revised form April 27*, *2015*)

In the present work, the entropy generation due to the heat transfer and fluid friction irreversibility is investigated numerically for a three-dimensional flow induced by rotating and stretching motion of a cylinder. The isothermal boundary conditions are taken into account for the heat transfer analysis. The similarity transformations are utilized to convert the governing partial differential equations to ordinary differential equations. Resulting nonlinear differential equations are solved using a numerical scheme. Expressions for the entropy generation number, the Nusselt number and the Bejan number are obtained and discussed through graphs for various physical parameters. An analysis has been made to compare the heat transfer irreversibility with fluid friction irreversibility using the expression of the Bejan number. It is found that the surface is a durable source of irreversibility and the curvature of cylinder is to enhance the fluid friction irreversibility.

Key words: swirling flow, stretching cylinder, entropy generation, heat transfer.

Introduction

Boundary layer flows and heat transfer over the stretching and rotating solid surfaces are the fields of great interest for scientists and engineers. In the production of various kinds of metallic and polymeric materials, such as metallic and plastic sheets, wires and fiber drawing, the raw material is melted under high temperature and passes through the die for extrusion process. Now, the material endures linear stretching, rotation, elongation and then cooled to solidify. Such kind of processes are very effective in production of plastic made equipment and fabrication of metallic, such as cutting tools, electronic components in a computer, rolling and annealing of copper wires etc. Due to these enormous implications in industrial, engineering and manufacturing processes, it has been gaining great attraction and curiosity of researchers from the hypothetical point of view. Furthermore, cooling of solid boundary is a basic tool to deal with the boundary layers in many engineering and industrial processes. Due to such realistic and practical impacts, the problem of cooling has been becoming an area of attention for scientists and engineers.

A solution of the cooling problem for flat plate was adduced for the first time in the article [1], where an expression for the heat transfer rate was formulated. The flow over moving solid surfaces was analyzed for the first time in the article [2]. The work was further extended in [3, 4] to analyze the thermal properties of flow. Flow over a stretching surface was discussed in the article [5], where an exact solution for the problem was obtained. The heat transfer effects on the flow over stretching surface were scrutinized in the article [6]. The work [5] was extended afterwards to three dimensional flows in [7] by assuming the sheet to be stretched in two perpendicular directions. The investigations [8–10] were devoted to the heat transfer effects over a stretching surface. The boundary layer flow in axial direction over the stretching cylinder with heat transfer analysis was studied in the work [11]. Subsequently, various authors [12–17] have further examined the numerous physical aspects of the idea of [11] and obtained similarity solutions over stretching cylinder. The exact solution for the axisymmetric flow near a stretching cylinder was obtained in [12]. The numerical solution by finite difference method for the heat transfer analysis of the flow over a stretching cylinder was obtained in [13]. The hydromagnetic flow due to porous stretching cylinder was examined in [14], and the authors of [15] presented the numerical solution using the Keller-box scheme. The authors of [16] inspected the stagnation point flow over a stretching cylinder and discussed the aligned and nonaligned streams of flow. Furthermore, the authors of [17] numerically investigated the heat transfer effect in the unsteady axial flow induced by a vertical rotating cylinder. Recently, the viscous flow over a stretching cylinder with torsion motion was discussed in [18] and a numerical solution was obtained.

The phenomenon of entropy generation has been studied widely by scientists and engineers due to the deficiency of energy capitals in all over the world. In fact, in numerous engineering processes the controlling of energy losses is admitted as a challenging problems to be dealt. Therefore, it is needed to develop such systems which utilize less energy resources and having good output performance. The entropy analysis of such systems is found to be helpful in improving thermal efficiency and minimizing power losses. Consequently, the study of entropy generation is a valuable tool to analyze the energy losses in the process of convective heat transfer.

Hypothetically, the second law analysis in convective heat transfer arrangements was initially studied in [19], where some methods to improve thermal efficiency of system were discussed. In another study [20], the entropy analysis in various flow configurations under the forced convection heat transfer was done and two main sources that produce the entropy, namely, the rate of heat transfer and the viscous effect of the fluid were investigated. Numerous investigations have been made on the work [20] to study the irreversible entropy generation in various convective heat transfer processes. The entropy analysis for the flow in an isothermal channel with heat mass transfer was done in [21]. The authors of [22] examined the entropy production in the flow over a rotating cylinder for different values of curvatures and noted that entropy generation increases as the Reynolds number increases. The entropy production in the flow of viscous fluid in annulus with rotating outer cylinder was analyzed in the work [23]. Furthermore, the authors of [24] analytically studied the irreversibility effects of hydromagnetic flow of a viscoelastic fluid over a stretching sheet. The authors of [25] conducted the entropy analysis for two sorts of convective heat transfer problems; namely, the flow in a channel consisting of two parallel plates and the flow in a channel with circular cross section. A complete thermodynamic analysis of the hydromagnetic flow in permeable channel was made in [26] analytically. The transverse magnetic field effect was also analyzed in [27] in a forced convection flow over a flat plate. The effect of slip condition on entropy generation in the hydromagnetic flow over a rotating disk was examined in the work [28]. The authors of [29] investigated the entropy generation in the flow in a porous medium over stretching plate using two kinds of boundary conditions, namely, prescribed surface temperature PST and prescribed heat flux PHF. Recently, the authors of the works [30] and [31] numerically discussed the phenomenon of entropy in unsteady flow over a stretching cylinder and showed that large curvature of cylinder results in increasing of irreversibility.

This work presents the first and second laws analyses of a three-dimensional flow over a rotating and stretching cylinder. For the heat transfer analysis, the surface of cylinder is assumed to be isothermal. The governing equations are solved numerically by the shooting method. The entropy analysis is made by using the second law, and the results are discussed by plotting graphs and tables for the various values of physical parameters.

Mathematical formulation

Consider the three-dimensional laminar boundary layer axial flow of a viscous fluid over a rotating stretchable cylinder of radius R. Assume that the surface of cylinder is being stretched along axial direction z, while r-axis is normal to the surface of cylinder. Furthermore, the cylinder is rotating about its axis $r = 0$ with constant angular velocity ω and held at the constant surface temperature T_w. For the axisymmetric flow, the variation with respect to the φ-coordinate is ignored. The axonometric illustration of the considered flow phenomenon is shown in Fig. 1. Under the above assumptions and considering the viscous dissipation the governing equations are

$$\partial u/\partial r + u/r + \partial w/\partial z = 0, \tag{1}$$

$$v^2/r = (1/\rho)(\partial p/\partial r), \tag{2}$$

$$u\frac{\partial v}{\partial r} + \frac{uv}{r} + w\frac{\partial v}{\partial z} = \nu\left(\frac{\partial^2 v}{\partial r^2} + \frac{1}{r}\frac{\partial v}{\partial r} - \frac{v}{r^2}\right), \tag{3}$$

$$u\frac{\partial w}{\partial r} + w\frac{\partial w}{\partial z} = -\frac{1}{\rho}\cdot\frac{\partial p}{\partial z} + \nu\left(\frac{\partial^2 w}{\partial r^2} + \frac{1}{r}\cdot\frac{\partial w}{\partial r}\right), \tag{4}$$

$$\rho C_p\left(u\frac{\partial T}{\partial r} + w\frac{\partial T}{\partial z}\right) = k\left(\frac{\partial^2 T}{\partial r^2} + \frac{1}{r}\cdot\frac{\partial T}{\partial r}\right) + \mu\left[\left(\frac{\partial v}{\partial r} - \frac{v}{r}\right)^2 + \left(\frac{\partial w}{\partial r}\right)^2\right], \tag{5}$$

with the boundary conditions

$$\begin{gathered} u(r,z) = 0,\ \ v(r,z) = \omega r,\ \ w(r,z) = az, \\ T(r,z) = T_w \quad \text{at} \quad r = R; \end{gathered} \tag{6}$$

$$\begin{gathered} v(r,z) = 0,\ \ w(r,z) = 0, \\ T(r,z) = T_\infty \quad \text{as} \quad r \to \infty, \end{gathered} \tag{7}$$

where ρ, C_p, μ, and k are the density, the specific heat, the viscosity and thermal conductivity of the fluid, respectively.

To normalize the above system of differential Eqs. (1)–(7) the following dimensionless quantities are used:

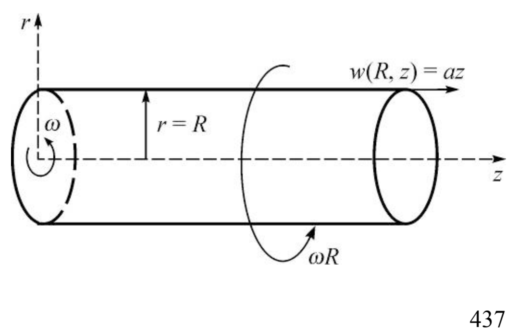

Fig. 1. View of the flow under study.

$$\begin{cases} u = -\dfrac{\sqrt{a\nu}}{r} F(\eta), \quad v = \omega R G(\eta), \quad w = azF'(\eta), \\ \theta = \dfrac{T - T_\infty}{T_\mathrm{w} - T_\infty}, \ \ p = \omega\rho\nu P(\eta), \quad \eta = \sqrt{\dfrac{a}{\nu}} \cdot \dfrac{r^2 - R^2}{2R}. \end{cases} \tag{8}$$

Equation (1) is satisfied identically, and after the passage to variables (8), one can rewrite equations (3)–(5) in the following form:

$$(1 + 2\kappa\eta)F''' + 2\kappa F'' + FF' - (F')^2 = 0, \tag{9}$$

$$(1 + 2\kappa\eta)^2 G'' + 2\kappa(1 + 2\kappa\eta)G' - \kappa^2 G + (1 + 2\kappa\eta)G'F + \kappa GF = 0, \tag{10}$$

$$(1 + 2\kappa\eta)\theta'' + 2\kappa\theta' + \Pr F\theta' = -\Pr(1 + 2\kappa\eta)\left[\mathrm{Ec}\left(G' - \frac{\kappa}{1 + 2\kappa\eta}G\right)^2 + \mathrm{Ec}_z (F'')^2\right], \tag{11}$$

subject to the boundary conditions

$$F(0) = 0, \ F'(0) = G(0) = \theta(0) = 1, \tag{12}$$

$$F'(\infty) = G(\infty) = \theta(\infty) = 0, \tag{13}$$

where F and G are the dimensionless velocity components in the direction of the r and φ axes, respectively, and equation (2) takes the following dimensionless form:

$$P'(\eta) = G^2 / (\kappa\Omega), \tag{14}$$

where $\kappa = (\nu/a)^{1/2}/R$ is the curvature parameter, $\Pr = \mu C_p/k$ the Prandtl number, $\mathrm{Ec} = (\omega R)^2/k\Delta T$ is the Eckert number due to rotation of cylinder, $\mathrm{Ec}_z = (az)^2/k\Delta T$ is the Eckert number due to stretching of cylinder, and $\Omega = a/\omega$ is the ratio between the stretching rate over the rate of angular velocity of cylinder.

The axial and tangential shear stresses τ_{rz} and $\tau_{r\theta}$ have the form:

$$\tau_{rz} = \mu \left.\frac{\partial w}{\partial r}\right|_{r=R} = \mu a \mathrm{Re}_z^{1/2} F''(0) \ \text{ and } \ \tau_{r\theta} = \mu \left.\frac{\partial v}{\partial r}\right|_{r=R} = \frac{\mu\Omega \mathrm{Re}_z^{1/2}}{\zeta} G'(0), \tag{15}$$

where $\zeta = z/R$ is the dimensionless axial coordinate, $\mathrm{Re}_z = az^2/\nu$ is the local Reynolds number. The full shear stress τ_w is defined as

$$\tau_w = \sqrt{\tau_{rz}^2 + \tau_{r\theta}^2}. \tag{16}$$

The skin-friction coefficient C_f reduces to

$$C_f = \frac{\tau_w}{\rho(az)^2} = \mathrm{Re}_z^{-1/2}\left((F''(0)^2 + \left(\frac{G'(0)}{\zeta\Omega}\right)^2\right)^{1/2}. \tag{17}$$

The heat transfer rate at the surface is calculated to be

$$q_\mathrm{w} = -k\left(\frac{\partial T}{\partial r}\right)_{r=R} = -k(T_\mathrm{w} - T_\infty)\left(\frac{a}{\nu}\right)^{1/2}\theta'(0), \tag{18}$$

and the local Nusselt number Nu takes the form

$$\mathrm{Nu} = \frac{q_\mathrm{w} z}{k(T_\mathrm{w} - T_\infty)} = -\mathrm{Re}_z^{1/2}\theta'(0). \tag{19}$$

Entropy analysis

To analyze the entropy production, it is supposed that the Fourier law of heat conduction is satisfied in the flow regime. As mentioned in [32], the local rate of entropy generation in cylindrical polar coordinates is given by

$$S_{\mathrm{G}} = \frac{k}{T_0^2}\left[\left(\frac{\partial T}{\partial r}\right)^2 + \left(\frac{\partial T}{\partial z}\right)^2\right] + \frac{\mu}{T_0}\left[\left(\frac{\partial v}{\partial r} - \frac{v}{r}\right)^2 + \left(\frac{\partial w}{\partial r}\right)^2\right]. \tag{20}$$

The above equation demonstrates two main causes of entropy production [32]. The first one is the heat conduction from surface to fluid and the second is the heat generated in fluid due to viscous dissipation. To normalize the above expression of the entropy generation, we use (8) and divide Eq. (20) by the characteristic entropy generation rate S_{G0} and get the total entropy generation number N_{G} as

$$N_{\mathrm{G}} = \alpha(\theta')^2 + \Pr(1+2\kappa\eta)\left[\mathrm{Ec}\left(G' - \frac{\kappa}{1+2\kappa\eta}G\right)^2 + \mathrm{Ec}_z\,(F'')^2\right], \tag{21}$$

where $\alpha = \Delta T/T_0$ is the dimensionless parameter and $S_{\mathrm{G0}} = ka\Delta T/(\nu T_0)$ is the characteristic entropy generation rate. In Eq. (21), the first term is the heat transfer irreversibility N_{H} due to the conduction through cylinder surface to the fluid, and the second term signifies the heat transfer irreversibility due to the viscous (or fluid friction) effects and is denoted by N_{F}. Thus, Eq. (21) can be written in the form

$$N_{\mathrm{G}} = N_{\mathrm{H}} + N_{\mathrm{F}}. \tag{22}$$

Another physical quantity of great interest is the Bejan number Be which is the ratio of the heat transfer irreversibility to the total entropy generation number and is defined as

$$\mathrm{Be} = N_{\mathrm{H}}/(N_{\mathrm{H}} + N_{\mathrm{F}}) = 1/(1+\phi), \tag{23}$$

where $\phi = N_{\mathrm{F}}/N_{\mathrm{H}}$ is the ratio between fluid friction entropy to the heat transfer entropy generation and mathematically can be expressed as

$$\phi = \frac{\Pr(1+2\kappa\eta)}{\alpha(\theta')^2}\left[\mathrm{Ec}\left(G' - \frac{\kappa}{1+2\kappa\eta}G\right)^2 + \mathrm{Ec}_z\,(F'')^2\right]. \tag{24}$$

From expression (23), it is noticed that the Bejan number is constrained in the range [0, 1]. In this range, the Bejan number demonstrates some special characteristics of fluid friction irreversibility in contrast with heat transfer irreversibility, which will be described briefly in the next section.

Results and discussion

The non-linear differential equations (9)–(11) along with the boundary conditions (12) and (13) are solved numerically using the shooting method. The semi-infinite domain is trimmed at the appropriate distance where the influence of boundary layer thickness is negligible. The built-in command of shooting method is used in the computational software Mathematica to solve the non-linear differential equations (9)–(13). During computations, the accuracy goal is adjusted to be 10^{-10}. In order to explore the physical effects of various imperative parameters the graphs are plotted in figures 2–13 for temperature, entropy generation, and other physical quantities.

Figure 2 illustrates the effects of curvature κ on the temperature profile. From the figure it can be observed that as κ increases the temperature profile increases. This conduct of the thermal boundary layer thickness is perceived because the heat transports in the fluid due to an enhanced convection process all around the cylinder. It is noticed from Fig. 3 that as Pr

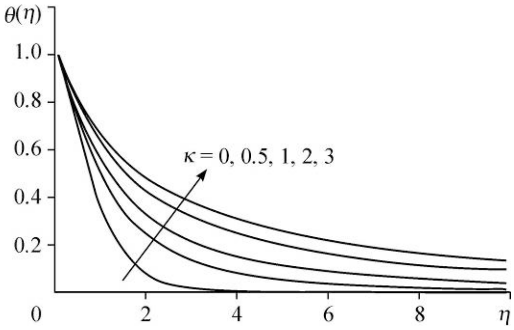

Fig. 2. Effect of curvature parameter κ on temperature profile $\theta(\eta)$ at constant criteria Pr = 2, Ec = Ec_z = 0.2.

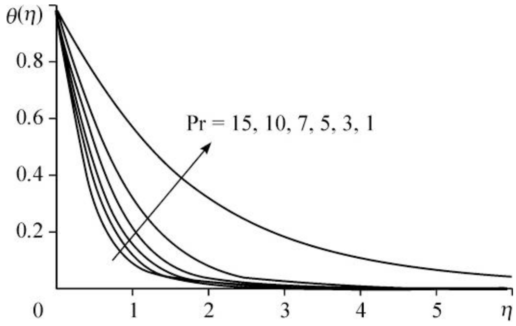

Fig. 3. Effect of Pr on temperature profile $\theta(\eta)$ at κ = Ec = Ec_z = 0.2.

increases the thermal layer thickness reduces rapidly and the effects of heat accumulates near to the surface of cylinder. It can also be examined from the figure that the fluids with the small Prandtl number impede the cooling process as compared to fluids having the large Prandtl number. This conduct of temperature profile shows that the Prandtl number is a main parameter that monitors the cooling process and therefore the fluids with high Prandtl number such as oils and lubricants are excellent coolants. The Table shows the effects of Pr and κ on the Nusselt number with isothermal boundary conditions. It is examined that the heat transfer rate increases as Pr increases which is because of the increasing temperature differences at the cylinder surface. It can also be noticed from the table that heat transfer rate decreases and deviates its sign as κ increases which shows the heat transfer from fluid to cylinder.

To examine the effects of Eckert numbers Ec and Ec_z on the temperature profile Figs. 4 and 5 are plotted, respectively. In both figures, the thermal boundary layer thickness increases by increasing the Eckert numbers, and the temperature of the fluid increases near the surface from the surface temperature. This is because of the large viscous resistance, more heat energy is accumulated in the fluid particles. However, the increase in temperature profile due to the rotating Eckert number Ec is more significant as compared to the stretching Eckert number Ec_z.

Table

Effect of the various parameters on the Nusselt number

κ	Pr	Ec	Ec_z	$-\theta'(0)$
0.0	2.0	0.2	0.2	0.65421
0.5	–	–	–	0.58756
2.0	–	–	–	0.02578
3.0	–	–	–	–0.43378
5.0	–	–	–	–1.41056
0.2	1.0	0.2	0.2	0.45527
–	3.0	–	–	0.76573
–	7.0	–	–	1.04595
–	10.0	–	–	1.16552
–	15.0	–	–	1.29375
–	1.0	0.0	–	0.54544
–	–	0.5	–	0.32000
–	–	1.0	–	0.09456
–	–	2.0	–	–0.35632
–	–	2.5	–	–0.58175
–	–	0.2	0.0	0.54790
–	–	–	0.5	0.31632
–	–	–	1.0	0.08475
–	–	–	1.5	–0.14683
–	–	–	2.5	–0.60998

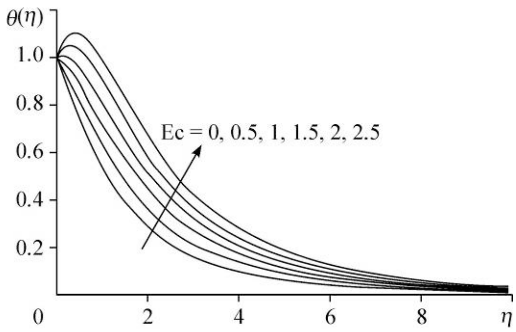

Fig. 4. Effect of Ec on the temperature profile $\theta(\eta)$ when $\kappa = \mathrm{Ec}_z = 0.2$ and Pr = 1 are fixed.

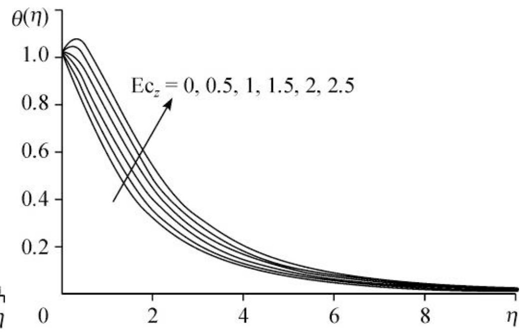

Fig. 5. Effect of Ec_z on the temperature profile $\theta(\eta)$ when $\kappa = \mathrm{Ec} = 0.2$ and Pr = 1 are fixed.

In the table, the numerical values of heat transfer rate for various values of Ec and Ec_z are listed. The rate of heat transfer decreases as the Eckert numbers increase, and for some moderate values of the Eckert numbers, the rate of heat exchange turns out to be negative.

The entropy generation number N_G which is a quantity of special interest to deduce the rate of irreversibility is plotted in Fig. 6. It is observed from the figure that an increase in κ results in an increment in N_G, and this increment is more significant near the surface of cylinder. It is observed from the figure that an increase in κ results in an increment in N_G and this increment is more significant near the surface of cylinder. This shows that the heat transfer irreversibility over slim cylinder is more considerable as compared to the plump cylinder or the flat plate, and also the surface acts as a strong source of irreversibility. The consequence of κ on the Bejan number is presented in Fig. 7. The common trend noticed in the figure is the decrease of Be in the vicinity of the surface and increase of Be far away from the surface as κ increases. It is also noticed that for small curvature the heat transfer irreversibility dominates over the fluid friction irreversibility and for large curvature the fluid friction irreversibility dominates. This is the consequence of decreasing velocity gradient for small curvature which results in decreasing entropy production due to viscous resistance in fluid. Another observation that can be observed from the figure is that the entropy production due to fluid friction dominates as one moves along the radial direction of cylinder. Obviously, this is due to the small temperature gradient in the ambient fluid where irreversibility is measured by viscous effects only.

The consequence of the Prandtl number Pr on the entropy production number N_G is illustrated in Fig. 8. It is noticed that Pr acts as a main cause of the entropy production and the entropy generation is more significant near the surface as compare to the main flow regime. Since both the velocity and temperature gradients are large near the surface therefore the discrimination of the strong irreversibility is only possible by plotting the Bejan number Be.

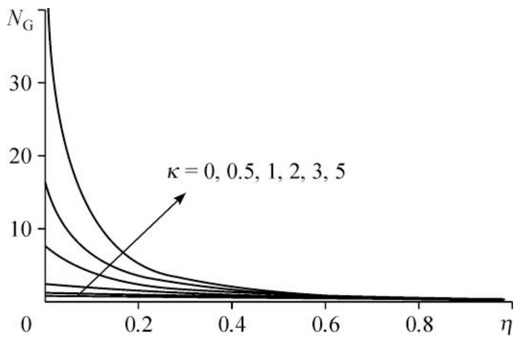

Fig. 6. Influence of κ on N_G when Pr = 1, $\mathrm{Ec} = \mathrm{Ec}_z = 0.2$ and $\alpha = 1$ are fixed.

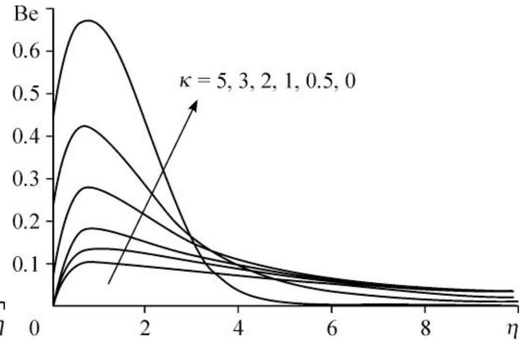

Fig. 7. Influence of κ on Be when Pr = 1, $\mathrm{Ec} = \mathrm{Ec}_z = 0.2$ and $\alpha = 1$ are fixed.

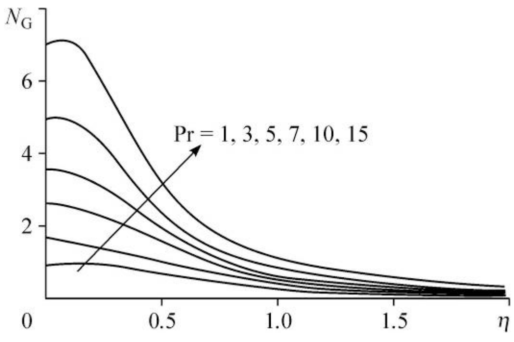

Fig. 8. Influence of Pr on N_G when κ = Ec = Ec_z = 0.2 and α = 1 are fixed.

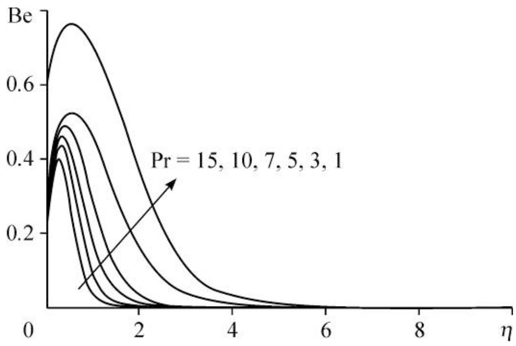

Fig. 9. Influence of Pr on Be wnen κ = Ec = Ec_z = 0.2 and α = 1 are fixed.

The Bejan number is plotted in Fig. 9 for different values of Pr and it is noticed that Be decreases as Pr increases. It is observed from the figure that the large Pr corresponds to the dominancy of fluid friction irreversibility.

Figures 10 and 11 show that the entropy production number N_G increases as the Eckert number Ec and Ec_z enhances. This is mainly because of augmentation of heat transfer due to viscous resistance of fluid particles. The graphs of the Bejan number for different values of Ec and Ec_z are plotted in Figs. 12 and 13 from where it is noticed that the increment in both the Eckert numbers strengthens the fluid friction irreversibility.

Conclusion

In this study, the second law of thermodynamic is applied to analyze the entropy generation in the boundary layer flow over a rotating stretchable cylinder. The heat transfer analysis is made using the isothermal boundary conditions. The governing equations are solved numerically using the shooting method. The obtained solution is utilized to investigate the entropy production due to the viscous dissipation and the heat transfer effects. It is seen that the involvement of curvature parameter is to increase the thermal boundary layer thickness, and the heat transfer rate decreases as the curvature of cylinder increases. It is found that the fluids with the large Prandtl number are excellent coolants, and the behavior of the Nusselt number shows that convection in the fluid with large Prandtl number is more efficient than that of the fluid with small Prandtl number. Increasing of curvature enhances the entropy generation, and also the large curvature plays a vital role in the augmentation of fluid friction irreversibility. Moreover, it is accomplished that the Prandtl and Eckert numbers are strong sources of fluid friction entropy production.

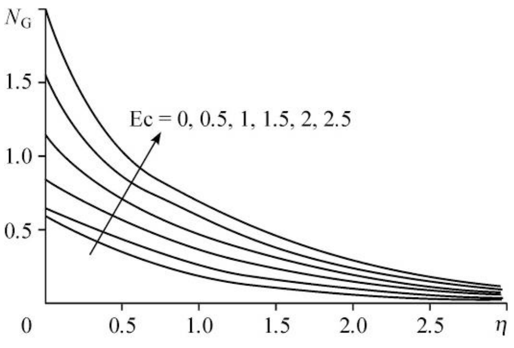

Fig. 10. Influence of Ec on N_G when Pr = 1, κ = Ec_z = 0.2, and α = 1 are fixed.

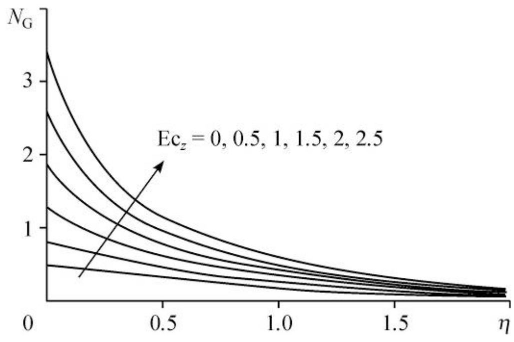

Fig. 11. Influence of Ec_z on N_G when Pr = 1, κ = Ec = 0.2, and α = 1 are fixed.

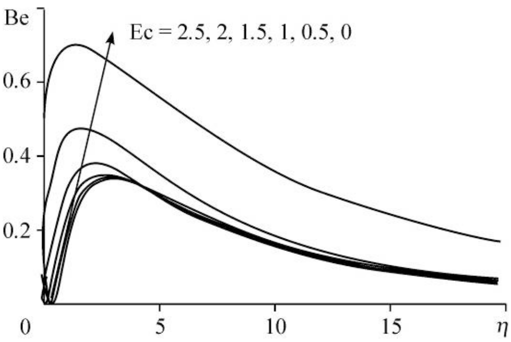

Fig. 12. Influence of Ec on Be when Pr = 1, κ = Ec_z = 0.2, and α = 1 are fixed.

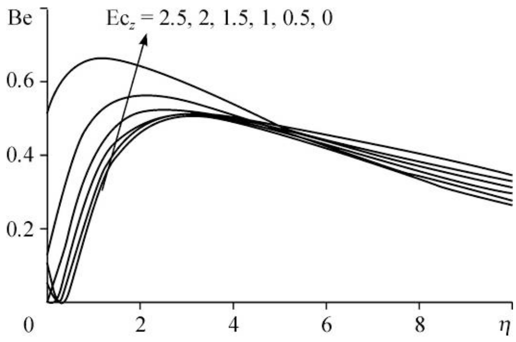

Fig. 13. Influence of Ec_z on Be when Pr = 1, κ = Ec = 0.2, and α = 1 are fixed.

References

1. **E. Pohlhausen,** Der Wärmeaustausch zwischen festen Körpern und Flüssigkeiten mit kleiner Reibung und kleiner Wärmeleitung, ZAMM-Z. Angew. Math. Mech., 1921, Vol. 1, No. 1, P. 115–121.
2. **B.C. Sakiadis,** Boundary-layer behavior on continuous solid surfaces. 1. Boundary-layer equations for 2-dimensional and axisymmetric flow, AIChE J., 1961, Vol. 7, P. 26–28.
3. **L.E. Erickson, L.C. Cha, and L.T. Fan,** The cooling of a moving continuous flat sheet, in AIChE Chemical Engng Process Symp., Eighth National Heat Transfer Conf., 1965, P. 157–165.
4. **F.K. Tsou, E.M. Sparrow, and R.J. Goldstein,** Flow and heat transfer in the boundary layer on a continuous moving surface, Int. J. Heat Mass Transfer, 1967, Vol. 10, No. 2, P. 219–235.
5. **L.J. Crane,** Flow past a stretching plate, Z. Angew. Math. Phys., 1970, Vol. 21, No. 4, P. 645–647.
6. **P. Carragher and L.J. Crane,** Heat transfer on a continuous stretching sheet, ZAMM-Z. Angew. Math. Mech., 1982, Vol. 62, No. 10, P. 564–565.
7. **C.Y. Wang,** The three-dimensional flow due to a stretching flat surface, Phys. Fluids, 1984, Vol. 27, P. 1915–1917.
8. **L.J. Grubka and K.M. Bobba,** Heat transfer characteristics of a continuous, stretching surface with variable temperature, J. Heat Transfer (Trans. ASME), 1985, Vol. 107, No. 1, P. 248–250.
9. **M.E. Ali,** Heat transfer characteristics of a continuous stretching surface, Wärmestoffübertrag., 1994, Vol. 29, No. 4, P. 227–234.
10. **E.M.A. Elbashbeshy,** Heat transfer over a stretching surface with variable surface heat flux, J. Phys. D: Appl. Phys., 1998, Vol. 31, No. 16, P. 1951–1954.
11. **C.Y. Wang,** Fluid flow due to a stretching cylinder, Phys. Fluids, 1988, Vol. 31. P. 466–468.
12. **G.I. Burde,** On the motion of fluid near a stretching circular cylinder, J. Appl. Math. Mech., 1989, Vol. 53, No. 2, P. 271–273.
13. **A. Ishak and R. Nazar,** Laminar boundary layer flow along a stretching cylinder, Eur. J. Sci. Res., 2009, Vol. 36, No. 1, P. 22–29.
14. **A. Ishak, R. Nazar, and I. Pop,** Uniform suction/blowing effect on flow and heat transfer due to a stretching cylinder, Appl. Math. Model., 2008, Vol. 32, No. 10, P. 2059–2066.
15. **A. Ishak, R. Nazar, and I. Pop,** Magnetohydrodynamic (MHD) flow and heat transfer due to a stretching cylinder, Energy Conv. Manag., 2008, Vol. 49, No. 11, P. 3265–3269.
16. **P.D. Weidman and M.E. Ali,** Aligned and nonaligned radial stagnation flow on a stretching cylinder, Eur. J. Mech. B / Fluids, 2011, Vol. 30, No. 1, P. 120–128.
17. **P.J. Singh, S. Roy, and I. Pop,** Unsteady mixed convection from a rotating vertical slender cylinder in an axial flow, Int. J. Heat Mass Transfer, 2008, Vol. 51, Nos. 5, 6, P. 1423–1430.
18. **T. Fang and S. Yao,** Viscous swirling flow over a stretching cylinder, Chin. Phys. Lett., 2011, Vol. 28, No. 11, P. 114702-1–114702-4.
19. **A. Bejan,** Second law analysis in heat transfer, Energy, 1980, Vol. 5, P. 720–732.
20. **A. Bejan,** A study of entropy generation in fundamental convective heat transfer, J. Heat Transfer. (Trans. ASME), 1979, Vol. 101, No. 4, P. 718–725.
21. **J.Y. San, W.M. Worek, and Z. Lavan,** Entropy generation in convective heat transfer and isothermal convective mass transfer, J. Heat Transfer (Trans. ASME), 1987, Vol. 109, P. 647–652.
22. **B.A.K. Abu-Hijleh and W.N. Heilen,** Entropy generation due to laminar natural convection over a heated rotating cylinder, Int. J. Heat Mass Transfer, 1999, Vol. 42, P. 4225–4233.
23. **B.S. Yilbas,** Entropy analysis of concentric annuli with rotating outer cylinder, Exergy Int. J., 2001, Vol. 1, P. 60–66.

24. **A.S. Butt, S. Munawar, A. Ali, and A. Mehmood,** Entropy analysis of mixed convective magnetohydrodynamic flow of a viscoelastic fluid over a stretching sheet, Z. Naturfors. Sect. A-J. Phys. Sci., 2012, Vol. 64, P. 451–459.
25. **S. Mahmud and R.A. Fraser,** The second law analysis in fundamental convective heat transfer problems, Int. J. Therm. Sci., 2003, Vol. 42, P. 177–186.
26. **S.H. Tasnim, M. Shohel, and M.A.H. Mamun,** Entropy generation in a porous channel with hydromagnetic effect, Exergy Int. J., 2002, Vol. 2, P. 300–308.
27. **M. Al-Odat, R. Damseh, and M. Al-Nimr,** Effect of magnetic field on entropy generation due to laminar forced convection past a horizontal flat plate, Entropy, 2004, Vol. 6, P. 293–303.
28. **A. Arikoglu, I. Ozkol, and G. Komurgoz,** Effect of slip on entropy generation in a single rotating disk in MHD flow, Appl. Energy, 2008, Vol. 85, P. 1225–1236.
29. **A. Tamayol, K. Hooman, and M. Bahrami,** Thermal analysis of flow in a porous medium over a permeable stretching wall, Transp. Porous Media, 2010, Vol. 85, P. 661–676.
30. **A.S. Butt and A. Ali,** Entropy analysis of magnetohydrodynamic flow and heat transfer due to a stretching cylinder, J. Taiwan Inst. Chem. Engng, 2014, Vol. 45, P. 780–786.
31. **S. Munawar, A. Ali, and A. Mehmood,** Thermal analysis of the flow over an oscillatory stretching cylinder, Phys. Scr., 2012, Vol. 86, No. 6, P. 065401.
32. **A. Bejan,** Entropy Generation Minimization, CRC Press, New York, Boca Raton, 1996.